We are IntechOpen, the world's leading publisher of Open Access books
Built by scientists, for scientists

6,900
Open access books available

186,000
International authors and editors

200M
Downloads

Our authors are among the

154
Countries delivered to

TOP 1%
most cited scientists

12.2%
Contributors from top 500 universities

CLARIVATE ANALYTICS

BOOK CITATION INDEX

INDEXED

WEB OF SCIENCE™

Selection of our books indexed in the Book Citation Index
in Web of Science™ Core Collection (BKCI)

Interested in publishing with us?
Contact book.department@intechopen.com

Numbers displayed above are based on latest data collected.
For more information visit www.intechopen.com

Effect of Flow Rate and Viscosity on Complex Fracture Development in UFM Model

Olga Kresse, Xiaowei Weng, Dimitry Chuprakov,
Romain Prioul and Charles Cohen

Additional information is available at the end of the chapter

http://dx.doi.org/10.5772/56406

Abstract

A recently developed unconventional fracture model (UFM*) is able to simulate complex fracture networks propagation in a formation with pre-existing natural fractures. Multiple fracture branches can propagate at the same time and crisscross each other. The behaviour of a hydraulic fracture when it intersects a natural fracture, whether being arrested, crossing, creating an offset, or dilating the natural fracture, plays a key role in predicting the resulting fracture footprint, microseismicity, and improving production evaluation. It is therefore critical to properly model the fracture interaction in a complex fracture model such as UFM.

A new crossing model, called OpenT, taking into account the effect of flow rate and fluid viscosity on the hydraulic/natural fracture crossing behaviour is integrated in UFM simulator. The previous fracture crossing model is primarily based on the stress field at the approaching hydraulic fracture tip and its interaction with the natural fracture. A new elasticity solution for the fracture contact has been developed. The new OpenT semi-analytical crossing model quantifies the localized stress field induced in the natural fracture and in the rock and evaluates the size and length of open and shear slippage zones along the natural fracture. The natural fracture activation and stress field near the intersection point are strongly dependent on the contacting hydraulic fracture opening and thus on fluid flow rate and viscosity. This new model is validated against laboratory experimental results and an advanced numerical model.

In this paper we present the results of several test cases showing the influence of injection rate and fluid viscosity on the generated hydraulic fracture footprint in formations with pre-

existing natural fractures. The influence of the stress field anisotropy, intersection angle, as well as natural fractures properties are also important and are discussed. The results are then compared with the simulations using the previous crossing model which does not account for the influence of fluid properties.

1. Introduction

It is believed that complexity of the fracture network created during hydraulic fracturing treatments in formations with pre-existing natural fractures is caused mostly by the interaction between hydraulic and natural fractures. The understanding and proper modelling of the mechanism of hydraulic-natural fractures interactions are keys to explain fracture complexity and the microseismic events observed during hydraulic fracturing treatments, and therefore to properly predict production.

When a hydraulic fracture (HF) intercepts a natural fracture (NF) it can cross the NF, open (dilate) the NF, or be arrested at NF. If the hydraulic fracture crosses the natural fracture, it remains planar, with the possibility to open the intersected NF if the fluid pressure at the intersection exceeds the effective stress acting on the NF. If the HF does not cross the NF, it can dilate and eventually propagate into the NF, which leads to more complex fracture network. So the crossing criterion in general controls the complexity of the resulting fracture network.

The interaction between HF and NF depends on the in-situ rock stresses, mechanical properties of the rock, properties of natural fractures, and the hydraulic fracture treatment parameters including fracturing fluid properties and injection rate. During the last decades, extensive theoretical, numerical, and experimental work has been done to investigate, explain, and develop the rules controlling HF/NF interaction. Among the main contributions to this topic are the work listed in references [1-15].

Most of the existing crossing models do not take into account fluid properties due to the complexity of modelling fluid-solid interaction in the vicinity of the intersection, so crossing behaviour is explained purely from elasticity point of view. Field and laboratory observations, however, show that fluid properties are important and should be accounted for [9, 16].

It is well known that the microseismic events cloud is related to the hydraulic fracture propagation pattern which in turn strongly depends on the HF/NF interaction rules [17].

Figure 1 shows the microseismic events observed in the same well first treated with a cross-linked gel, and then re-fractured with slick water [16]. Cross-linked gel was pumped at 70 bpm for about 3 hours with sand concentration ramped up to 3 ppg. Most of the microseismic activity suggests longitudinal fracturing with only modest activation of natural fractures, resulting in a narrow stimulated network (less than 500 feet from the wellbore in many sections of the lateral), as seen in Figure 1a with resulting Stimulated Reservoir Volume (SRV) equal to 430 million ft³. During the full re-frac conducted the following day 60,000 bbl of slick water and 285,000 lb of sand was pumped at 125-130 bpm for most of the treatment lasting 6.5 hours.

The stimulated network was approximately 1500ft wide and 3,000 ft long (Figure 1b) with considerable height growth and SRV of 1450 million ft³. Clearly, the re-fracturing treatment stimulated a much larger volume of rock than the initial gel treatment (1450 million ft³ vs 430 million ft³), and showed the patterns of development that suggested the opening of both northeast and northwest trending fractures [16].
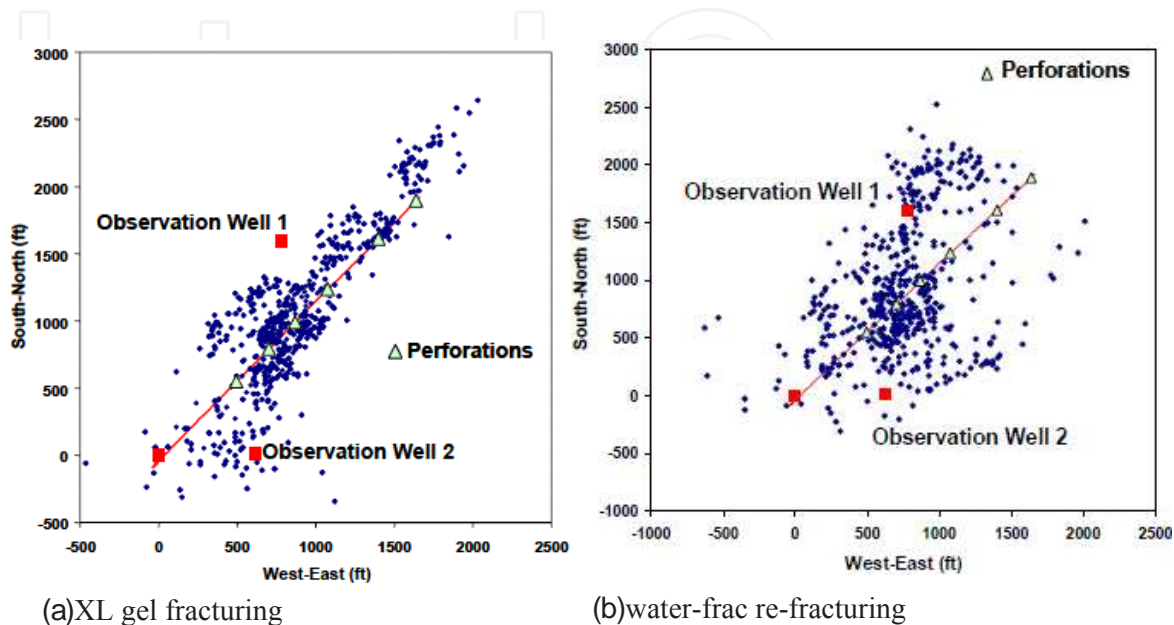

(a)XL gel fracturing   (b)water-frac re-fracturing

Figure 1. Single-well microseismic event locations for XL gel stimulation and water-frac re-fracturing treatment, horizontal Barnett Shale well [16]

This field example indicates the importance of proper consideration of fluid properties when modelling the interaction of hydraulic fractures with pre-existing natural fractures. In general it is observed that for the same field conditions more viscous fluid tends to cross the natural fractures more easily, while slick water tends to penetrate into the natural fractures more easily and open them without crossing. Pumping rate as well as rock properties should also be taken into account.

The importance of fluid properties on the created hydraulic fracture network has been mentioned in some experimental and numerical studies [9, 18, 19]. The experimental study of the influence of flow rate and fracturing fluid viscosity on the hydraulic fracture geometry have been performed in [9] based on analysis of different $Q\mu$ value (product of the injection rate and fracturing fluid viscosity). The experiments show that with low $Q\mu$ value fluid tends to leak into the pre-existing discontinuities despite the influence of fluid pressure and once the discontinuity accepts fluid, the pressure can rise far above the confining stress without inducing new fractures. With large $Q\mu$ value the hydraulic fracture tends to cross natural fracture due to increase of the pressurization rate.

The influence of fluid injection rate and viscosity on the amount of the tensile failure in the rock with natural fractures has been investigated based on 3DEC DEM model in [18, 19]. For low viscosity fluid the amount of area failing in shear is dramatically higher than in the case

with high viscosity. Their results show that an increase in injection rate greatly increases the amount of tensile failure within the model leading potentially to creating more fractures, while a lower injection rate favours the creation of shear failure resulting mostly in activating (opening) pre-existing natural fractures.

A new analytical model, called OpenT, for hydraulic fracture interaction with a pre-existing discontinuity has been developed to predict the fracture crossing or deflection at the encountered interface [20, 21]. The new physically rigorous criterion of fracture re-initiation at the discontinuity has been implemented, which combines both stress criterion and energy release rate. It has been shown that the OpenT model adequately predicts the fracture crossing of non-cohesive frictional interfaces observed in various laboratory experiments with different interface orientations with respect to hydraulic fractures [21].

The new crossing model predicts the dimensions of open and sliding zones created at cohesive and non-cohesive interfaces after the intersection with a fluid-driven fracture. Such information can be valuable, for example, in passive microseismic monitoring of fracture treatments in naturally fractured formations. By thoroughly examining the stress field generated by the hydraulic fracture and activated open and sliding zones at the discontinuity, it was shown that the new fracture initiation point is shifted along the inclined interface. The model predicts the offset of a secondary fracture as a function of the geometrical, loading, and mechanical parameters of the system, such as the fracture-interaction angle, in-situ stress components and fracture toughness in rock.

New OpenT crossing model incorporates the influence of rock properties (local horizontal stresses, rock tensile strength, toughness, pore pressure, Young's modulus, Poisson ratio), natural fracture properties (friction coefficient, toughness, cohesion, permeability), intersection angle between hydraulic and natural fractures, fracturing fluid properties (viscosity, tip pressure), and injection rate to define crossing rules.

This new OpenT model has been validated against laboratory experiments and against rigorous numerical models [3,20,21]. It was incorporated into the UFM model that simulates complex fracture network propagation in a formation with pre-existing natural fractures [22-24]. We present several UFM test cases showing the influence of injection rate and fluid viscosity on the generated hydraulic fracture footprint and production impact by comparing of two crossing criteria, the extended Renshaw & Pollard (hereafter referred as eRP) [14, 15] and the OpenT.

2. UFM model specifics

A complex fracture network model, referred to as Unconventional Fracture Model (UFM), had recently been developed [22,23,24]. The model simulates the fracture propagation, rock deformation, and fluid flow in the complex fracture network created during a fracture treatment. The model solves the fully coupled problem of fluid flow in the fracture network and the elastic deformation of the fractures, which has similar assumptions and governing

equations as conventional pseudo-3D fracture models. Transport equations are solved for each component of the fluids and proppants pumped. A key difference between UFM and the conventional planar fracture model is being able to simulate the interaction of hydraulic fractures with pre-existing natural fractures, i.e., determine whether a hydraulic fracture propagates through or is arrested by a natural fracture when they intersect and subsequently propagates along the natural fracture.

To properly simulate the propagation of multiple or complex fractures, the fracture model takes into account the interaction among adjacent hydraulic fracture branches, often referred to as "stress shadow" effect. It is well known that when a single planar hydraulic fracture is opened under a finite fluid net pressure, it exerts a stress field on the surrounding rock that is proportional to the net pressure. The details of stress shadow effect implemented in UFM are presented in [24].

The branching of the hydraulic fracture at the intersection with the natural fracture gives rise to the development of a complex fracture network. A crossing model that is extended from the Renshaw-Pollard [10] interface crossing criterion, applicable to any intersection angle, has been developed [14], validated against the experimental data [15], and was integrated in the UFM. The previous crossing model, showing good comparison with existing experimental data, does not account for the fluid impact on the crossing pattern.

The new crossing model (OpenT) which accounts for the fluid properties is presented in short below and is implemented in a new version of UFM.

3. New crossing model in UFM

There are a few analytical criteria describing the mechanical HF-NF interaction developed in the past [10, 11, 13, 14]. With their relative simplicity they do not take into account the influence of the fluid injection into the hydraulic fracture and the fluid infiltration into the natural fracture after contact. These criteria were designed to capture the effect of the fracture approach angle, the NF friction coefficient and the anisotropy of the in-situ stresses. To improve the description of HF-NF interaction a new analytical model that takes the mechanical influence of the HF opening and the hydraulic permeability of the NF into account has been developed.

The analytical model of the HF-NF interaction (OpenT) solves the problem of the elastic perturbation of the NF at the contact with the blunted HF tip, which is represented by a uniformly open slot (i.e. giving its name OpenT) [21]. The opening of the HF at the junction point w_T (blunted tip) develops soon after contact, and approaches the value of the average opening of the hydraulic fracture $\bar{w}$, defined by the injection rate Q and the fluid viscosity μ. In a viscosity-dominated regime, the average opening of the KGD fracture with half-length L and height H can be estimated as [25]

$$\bar{w} = 2.53\left[\frac{Q\mu L^2}{E'H}\right]^{1/4}$$

(1)

where $E' = E/(1-\nu^2)$, E is the Young modulus, ν is the Poisson coefficient. The OpenT model looks for the solution of the elastic problem for the NF perturbed by the HF, and outputs the profiles and boundaries of the opening and sliding zones as a result of the contact (b_o and b_s respectively shown in Figure 2, left).

The solution shows that the spatial extent of the open and sliding zones strongly depends on the fluid pressure inside the activated part of the NF. The larger the inner fluid pressure, the larger the open and sliding zones at the NF are. Consequently, it is expected that after the HF-NF contact, the injected fracturing fluid will gradually penetrate the NF with finite hydraulic permeability κ and thus enhance the inner fluid pressure within the NF, p_{NF}.
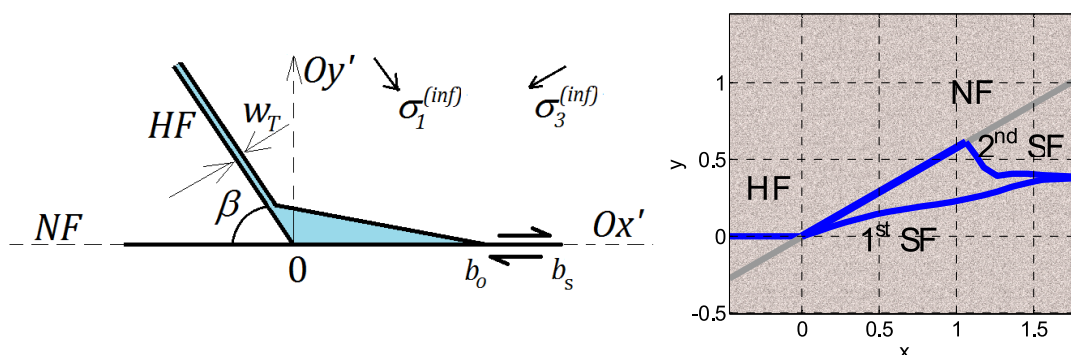

Figure 2. Left –Schematic diagram of the HF-NF interaction. Right – result of the computed HF/NF interaction with the initiation of two secondary fractures and their subsequent propagation

The average pressure of the fracturing fluid penetrated the NF can be as approximated by the following function of the contact time t

$$p_{NF}(t) = p_f \tanh\left(\sqrt{\frac{2\kappa p_f}{\mu b_s^2}t}\right)$$

(2)

where p_f is the fluid pressure at the contacting HF tip. As a result of the NF activation due to the fracturing, the fluid penetration becomes very active in highly permeable NFs or with low viscosity fracturing fluids. This could potentially prevent the HF from propagation across the weak interfaces.

The elasticity model of the fracture interaction enables the computation of the stress field in the vicinity of the activated NF. The analysis of the generated stress field gives the positions of sufficient tensile stress concentration where the new fractures can be nucleated. These

positions in most situations correspond to the two opposite tips of the NF open zone (see Figure 2, right). In order to decide on the possibility of a secondary fracture (SF) re-initiation at these points, a criterion of fracture initiation which combines both stress criterion and energy release rate has been employed. The stress criterion requires that the maximum tensile hoop stress $\sigma_{\theta\theta}$ in the vicinity of the stress concentration point x_j having direction θ_j with respect to the orientation of the NF must exceed the tensile strength of the rock T_0 along the distance δ_T

$$\sigma_{\theta\theta}(x_j, r, \theta_j)_{r<\delta_T} \leq -T_0$$

(3)

In addition, the energy criterion states that the elastic energy release rate due to the incremental initiation of a fracture of length δl must overcome the critical energy release rate for the given rock

$$\Im_{inc}(\delta l) > \Im_{1C}, \quad \delta l < \delta_T$$

(4)

The length of the fracture must not exceed the critical stress zone, δ_T. The mixed stress-energy criterion has been verified experimentally [26].

The model of HF-NF re-initiation has been validated against the results of various laboratory block tests [11, 12, 15]. The predictions of the analytical model for crossing and arresting behaviour agree with the experimental results for various fracture intersection angles, stress contrasts and fluid injection conditions used in different experimental groups. Figure 3 shows the comparison between different analytical models [13, 14, 21], and the experimental results from [15].

The experiments clearly show that the new model agrees with the experiments as well as other analytical models as it captures the first order crossing-arresting behavior. We note that the discrimination between the different models would require additional data points in the transition zone, unfortunately not available here.

Additionally, it should be noted that the injection rate and viscosity were not changed in this series of experiments, and so it was not possible to assess their effect on the fracture interaction outcome. In order to compensate for this lack of lab experiments, numerical experiments were conducted using MineHF2D code [4, 5, 8] to assess the sensitivity of the injection rate on fracture crossing. The results are demonstrated on Figure 4 and show that the OpenT model [20,21] agrees well with numerical computation results in the sense that it captures the crossing-arresting transition.

It should be mentioned that the OpenT incorporates the influence of rock properties (local horizontal stresses, rock tensile strength, toughness, pore pressure, Young's modulus, Poisson ratio), natural fracture properties (friction coefficient, toughness, cohesion, permeability), intersection angle between hydraulic and natural fractures, fracturing fluid properties (viscosity, tip pressure), and injection rate to define crossing rules [21]. The eRP criterion

[14,15] accounts for the local stress field, pore pressure, crossing angle, rock tensile strength and frictional properties of the natural fractures.
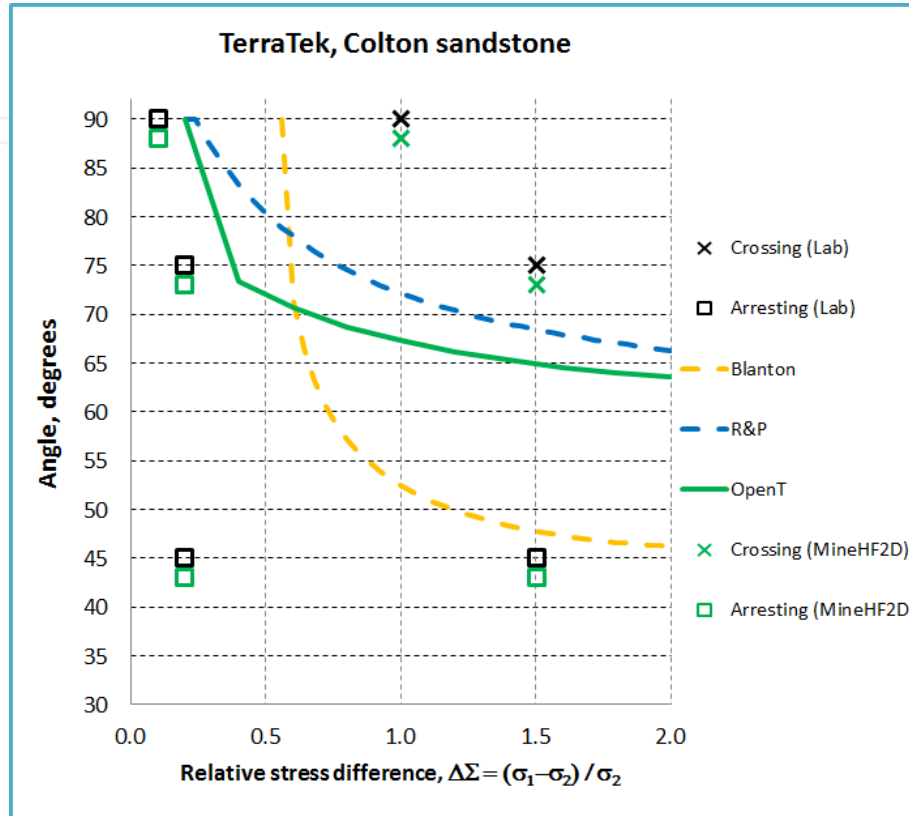

Figure 3. Comparison between analytical models given in [13,14,15], OpenT [21], and the experimental results [15]
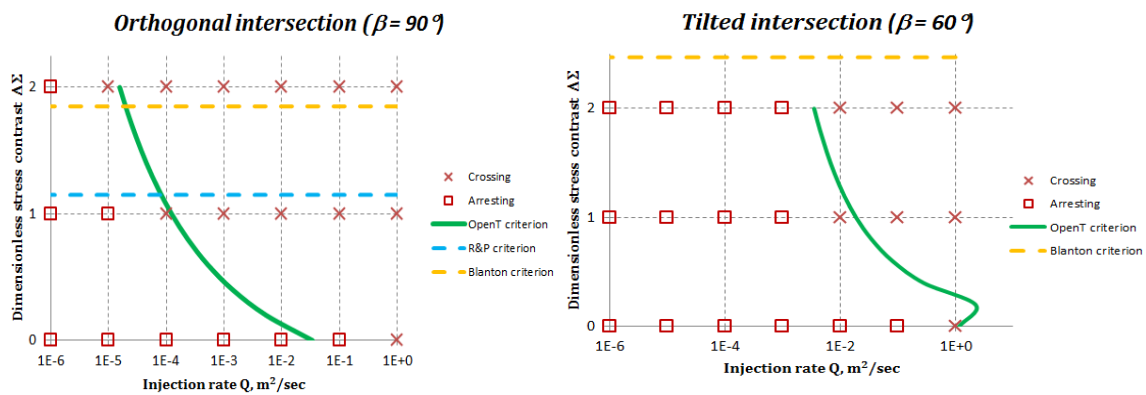

Figure 4. Comparison between numerical crossing-arresting HF-NF behavior using MineHF2D code [4,5,8]. The red crosses and squares respectively indicate crossing and arresting behavior from MineHF2D code, solid green curves correspond to analytical predictions using OpenT [21], dash yellow curve corresponds to Blanton criterion [13], and eRP criterion [14,15] is given by dash blue lines. The interaction is studied for various injection rate and relative stress difference for two different HF-NF contact angles, β=90⁰ (left) and β=60⁰ (right).

This new model has been implemented in UFM. Below we present comparison of UFM results with new and old crossing models and provide some analysis about the influence of fluid properties on the geometry of stimulated fracture network, and as a result on the production predictions.

4. Comparison of hydraulic fracturing simulations with OpenT versus eRP

4.1. Influence of viscosity

The comparison of results generated using two crossing criteria - eRP criterion [14,15] and new OpenT criterion [20, 21] - is presented in Figure 5 and Figure 6 for a simple example given in Table 1 (values shown in italic are used only in OpenT crossing criterion). The cohesion and toughness of natural fracture are considered to be negligible.

Injection rate	0.13 m³/s
Stress anisotropy	0.9 MPa
Young's modulus	2.8×10^{10} Pa
Poisson's ratio	0.2
Fluid viscosity	0.001-0.01 Pa-s
Fluid Specific Gravity	1.0
Fracture toughness	1.3 MPa-m$^{0.5}$
Tensile strength	3.5 MPa
NF friction Coefficient	0.5
NF permeability	1 Darcy

Table 1. Input data Example 1

For the case of lower fluid viscosity (Figure 5a and Figure 6a) both criteria show similar hydraulic fracture patterns with no crossing of the natural fractures. For higher viscosity fluid OpenT crossing criterion shows that hydraulic fractures cross the NF#1 and NF#3 (Figure 6b), while with eRP the hydraulic fracture network (HFN) pattern does not change. The intersection angle between HF and NF#1 was 62.5 deg, between HF and NF#2 was 15 deg, and the interaction angle between HF and NF#3 was 75 deg.
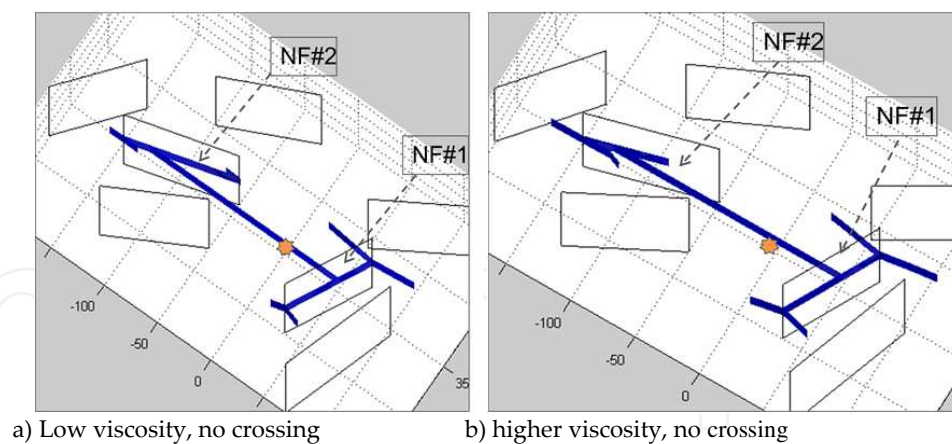
a) Low viscosity, no crossing   b) higher viscosity, no crossing

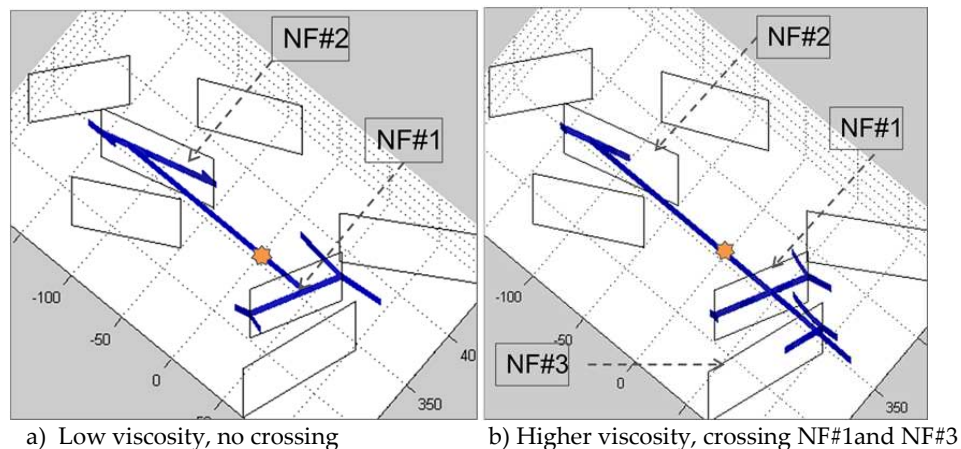**Figure 5.** Hydraulic fracture networks generated for Example 1 with eRP crossing criterion [14] with fluid viscosity K'=0.001Pa-s (left), and K'=0.01Pa-s (right)

a) Low viscosity, no crossing   b) Higher viscosity, crossing NF#1and NF#3

Figure 6. Hydraulic fracture networks generated for Example 1 with OpenT crossing criterion [21] with fluid viscosity K'=0.001pa-s (left) and K'=0.01Pa-s (right)

So, while eRP criterion gives for this case the same prediction (no crossing) for both low and high viscosity fluids, OpenT criterion predicts crossing the NF with higher crossing angle for the more viscous fluid.

Differences in the predicted hydraulic fracture network result in different proppant placement (Figure 7), and will result in differences in production evaluation and prediction.

Example 2 with more dramatic output differences is presented in Figure 8 for the same pumping schedule, zone properties, fluid and natural fractures properties. In Table 2 the main input data is shown (values shown in italic are used only in OpenT crossing criterion), the toughness and cohesion of natural fractures are considered to be negligible. Natural fractures are oriented mostly perpendicular (~ 90deg) to the maximum horizontal stress direction, i.e. to the preferred direction of hydraulic fracture propagation.
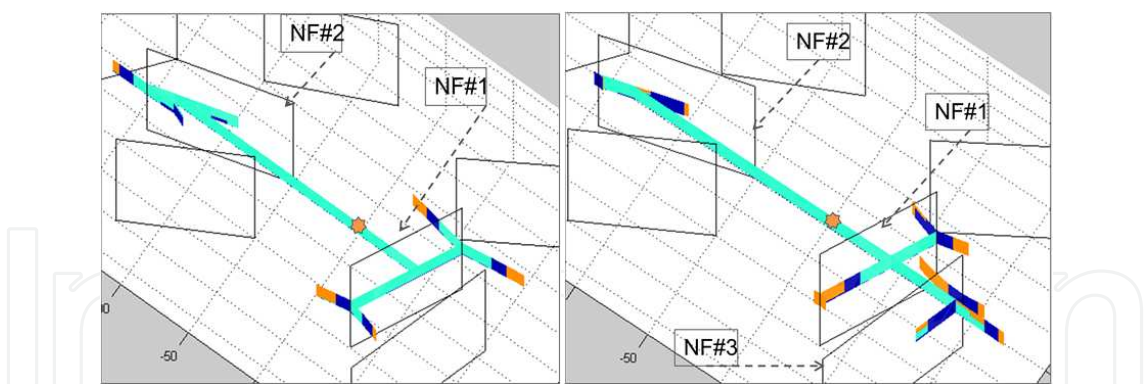
Figure 7. Proppant placement prediction for Example 1 from eRP (left) and OpenT (right) criteria with fluid K'=0.01Pa-s after 100 min of shut-in. Slurry is shown in light blue, bank is in dark blue, and clean fluid is in orange.

Injection rate	0.13 m³/s
Stress anisotropy	2 MPa
Young's modulus	$3.5×10^{10}$ Pa
Poisson's ratio	0.25
Fluid viscosity	0.0004-0.04 Pa-s
Fluid Specific Gravity	1.0
Min horizontal stress	42.7 MPa
Max horizontal stress	44.6 MPa
Fracture toughness	1 MPa-m$^{0.5}$
Tensile strength	3.4 MPa
NF friction Coefficient	0.4
NF permeability	1 Darcy

Table 2. Input data for Example 2

For the case of low viscosity fluid (Figure 8 left) both criteria show similar hydraulic fracture patterns with mostly no crossing of the natural fractures. When fracturing fluid viscosity was increased, considerable differences in patterns have been observed (Figure 8 right). The results for eRP approach stay mostly the same, showing that fluid eventually penetrated into the NF and opens it. But the simulation based on OpenT criteria shows that for higher viscosity fluid hydraulic fracture intersects most of the natural fractures, resulting in a bi-wing like HFN pattern, which will produce a narrow microseismic events cloud.

The example presented on Figure 8b is consistent with the general observations that hydraulic fracturing treatments with higher fluid viscosity HFN tend to cross natural fractures and

generate a narrower fracture network, while for low viscosity fluids it is easier to penetrate into the natural fracture and open it [9] and generate a wider fracture network.
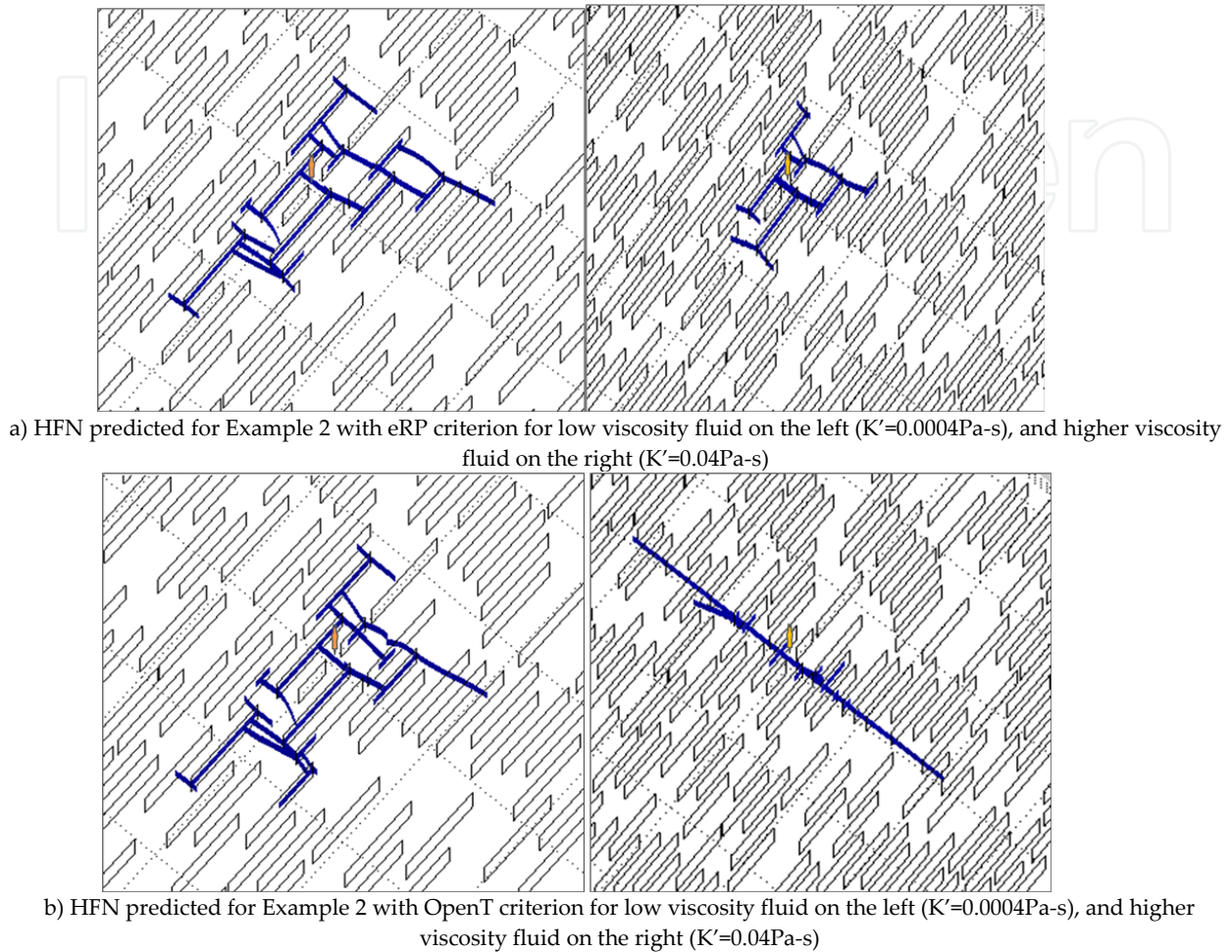

a) HFN predicted for Example 2 with eRP criterion for low viscosity fluid on the left (K'=0.0004Pa-s), and higher viscosity fluid on the right (K'=0.04Pa-s)

b) HFN predicted for Example 2 with OpenT criterion for low viscosity fluid on the left (K'=0.0004Pa-s), and higher viscosity fluid on the right (K'=0.04Pa-s)

Figure 8. Hydraulic fracture networks generated for Example 2 with eRP crossing criterion (a) and OpenT crossing criterion (b) for low and high fluid viscosity cases. The pre-existing DFN is also shown

It should be mentioned that rock properties, crossing angle between natural fracture and hydraulic fracture, and natural fractures properties all work together with fluid properties to define the crossing pattern and the resulting fracture footprint. This paper intends to emphasize the importance of fluid properties to be included into the general consideration for HF/NF interaction prediction.

4.2. Influence of pumping rates

As it was mentioned before, injection rate works together with fluid viscosity when HF interacts with NF [9, 18, 19]. In the OpenT crossing model the injection rate is also taken into account to predict (evaluate) HF/NF crossing or opening (Equation 1).

Notice that while using eRP criterion, the change in pumping rate can change fracture footprint due to change in fluid pressure, width, and therefore local stresses and crossing angle, while OpenT model introduces additional change due to the rate effect on the crossing behaviour.

The cases presented in Examples 1-2 above, demonstrated the impact of fluid viscosity. Now these examples will be considered again to demonstrate the impact of pumping rate, which is also accounted for in the new crossing model. The base case of pumping rate Q=0.132 m³/s is considered and compared with additional cases when rate is changed (Table 3). The total pumping time in schedule was changed accordingly for different pumping rates to maintain the same total fluid volume.

Fluid viscosity	0.0004-0.04 Pa-s
Injection rate : Q	0.132 m³/s
Injection rate: Q/2	0.066 m³/s
Injection rate: 5Q	0.66 m³/s

Table 3. Input data to test impact of pumping rate

First, on Figures 9a-10a the results of using the eRP crossing model with different rates as given in Table 3, and two types of fluid viscosity are presented for Example 1 and compared with the same simulations using OpenT crossing model (Figures 9b-10b). Due to relatively high leakoff coefficient used in the presented case the fracture network for higher rate is larger due to greater fluid efficiency.
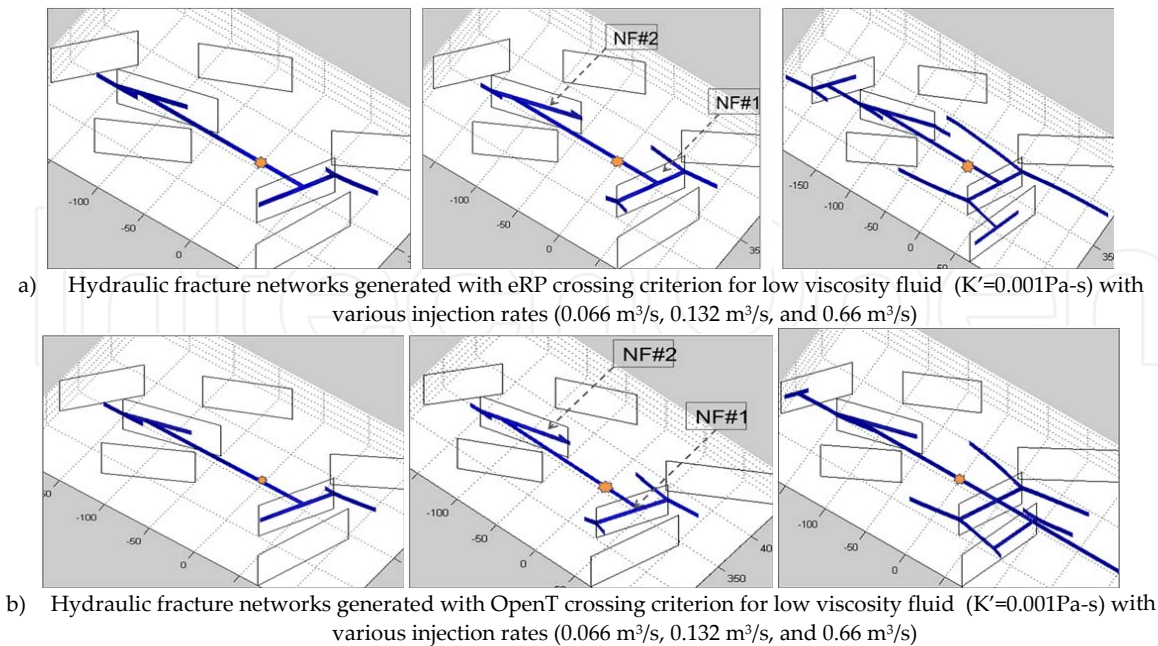

a)   Hydraulic fracture networks generated with eRP crossing criterion for low viscosity fluid (K'=0.001Pa-s) with various injection rates (0.066 m³/s, 0.132 m³/s, and 0.66 m³/s)

b)   Hydraulic fracture networks generated with OpenT crossing criterion for low viscosity fluid (K'=0.001Pa-s) with various injection rates (0.066 m³/s, 0.132 m³/s, and 0.66 m³/s)

Figure 9. Influence of Pumping Rate: Hydraulic fracture networks generated for Example 1 with low viscosity fluid and with eRP (a) and OpenT(b) crossing models at injection rates from Table 3
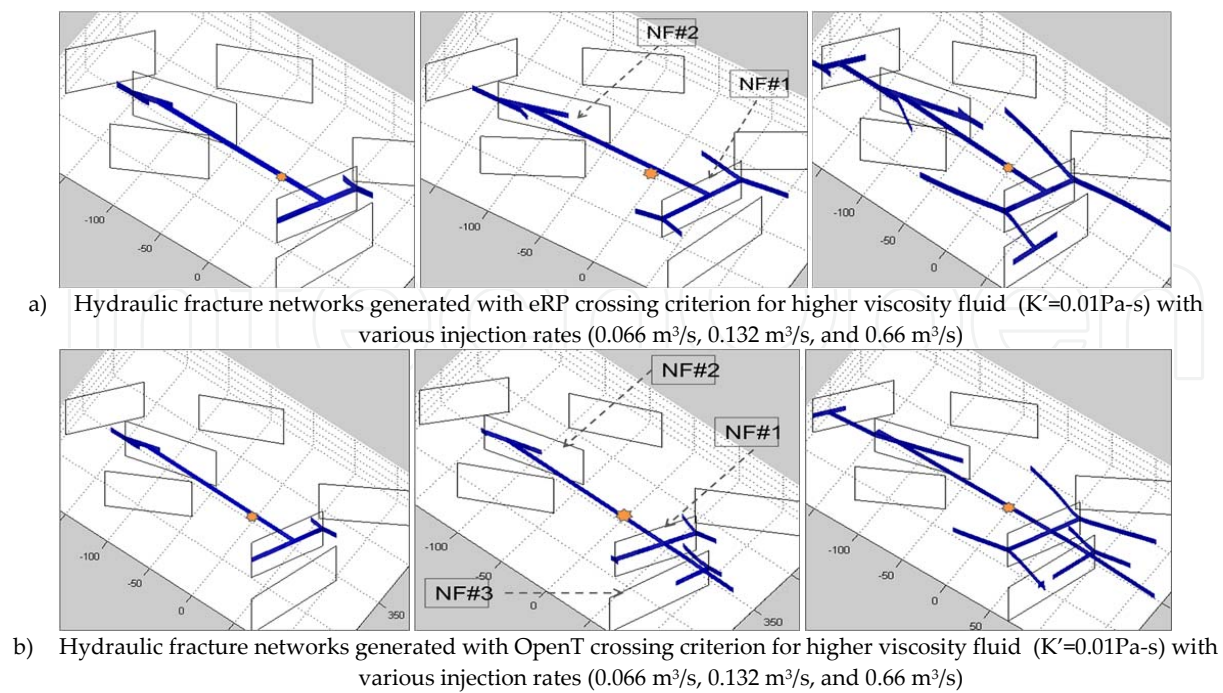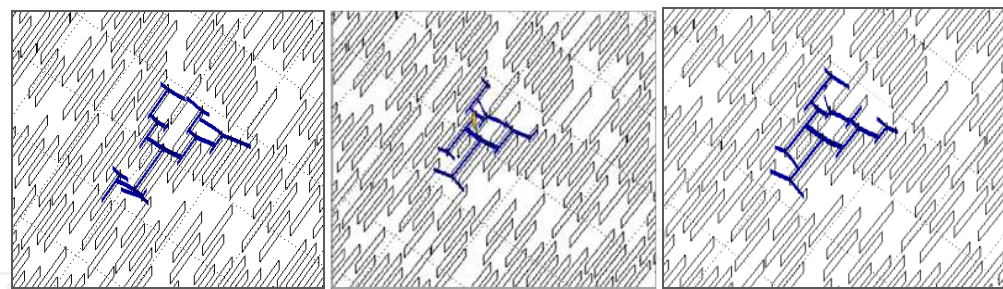
a)   Hydraulic fracture networks generated with eRP crossing criterion for higher viscosity fluid (K′=0.01Pa-s) with various injection rates (0.066 m³/s, 0.132 m³/s, and 0.66 m³/s)

b)   Hydraulic fracture networks generated with OpenT crossing criterion for higher viscosity fluid (K′=0.01Pa-s) with various injection rates (0.066 m³/s, 0.132 m³/s, and 0.66 m³/s)

Figure 10. Influence of Pumping Rate: Hydraulic fracture networks generated with higher viscosity fluid for Example 1 with eRP (a) and OpenT(b) crossing models at injection rates from Table 3

The first observation is that for low injection rate and for both high and low fluid viscosities fracture network is similar with both crossing models for this simple Example 1, and no crossing is observed. When injection rate is increased, HFN becomes more complex: OpenT shows crossing at the first natural fracture at the angle of 62.5 deg with both low and high viscosity fluids. The eRP criterion does not show crossing, and network complexity is due to the smaller time required to open NF and higher injection rates, so HFN can propagate faster. Again, the resulting HFN with eRP model does not depend on the fluid viscosity (Figure 9a and Figure10a). Results for the test case of Example 2 are given in Figures 11-12.
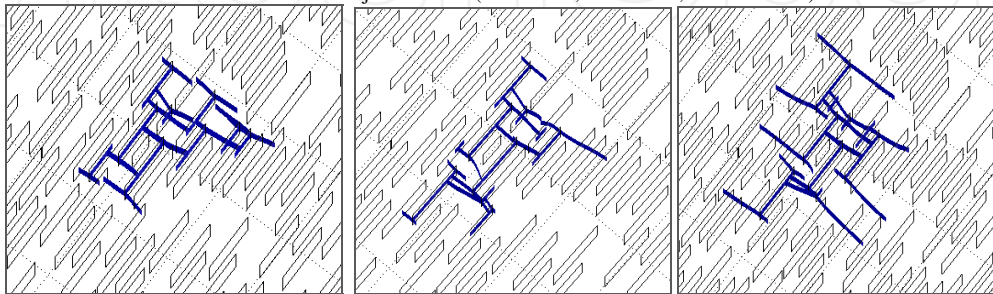
As we can see from Figures 11a and 12a, eRP criterion exhibits similar HFN footprints for both low and high viscosity fluids and for different injection rates. The reason for the relative insensitivity to the injection rate as compared to Example 1 is due to the higher stress aniso-tropy for Example 2.

With OpenT crossing criterion, for lower fluid viscosity the chance of crossing perpendicular NF increases with increasing injection rate. At the same time for a higher viscosity fluid, while it can cross the natural fracture more easily, it is more difficult to open the crossed natural fracture. The observed behaviour with new crossing model is consistent with experimental observations [9].

So we can conclude from the observations in these cases that the fluid viscosity together with pumping rate could play a major role on the crossing. At the same time the influence of pumping rate is not as strong as viscosity, and mostly affects the opening of the intersected natural fractures.
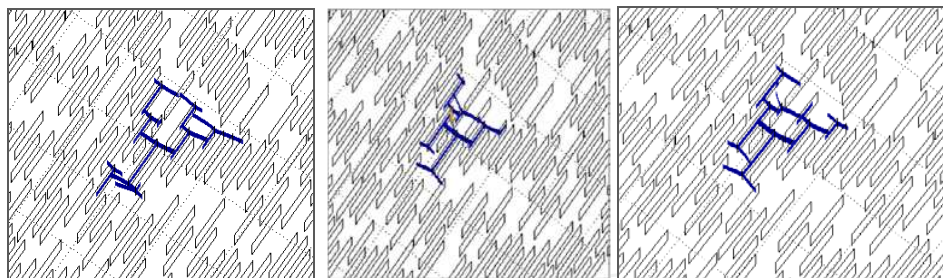
a)   Hydraulic fracture networks generated with eRP crossing criterion for low viscosity fluid (K'=0.0004Pa-s) with various injection rates (0.066 m³/s, 0.132 m³/s, and 0.66 m³/s)
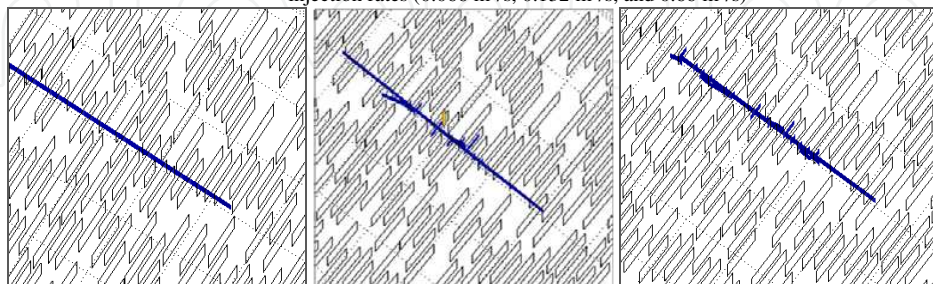

b)   Hydraulic fracture networks generated with OpenT crossing model for low viscosity fluid (K'=0.0004Pa-s) with various injection rates (0.066 m³/s, 0.132 m³/s, and 0.66 m³/s)

Figure 11. Influence of Pumping Rate: Hydraulic fracture networks generated with low viscosity fluid for Example 2 with eRP (a) and OpenT(b) crossing models at injection rates from Table 3

a)   Hydraulic fracture networks generated with eRP crossing model for higher viscosity fluid (K'=0.04Pa-s) with various injection rates (0.066 m³/s, 0.132 m³/s, and 0.66 m³/s)

b)   Hydraulic fracture networks generated with OpenT crossing model for higher viscosity fluid (K'=0.04Pa-s) with various injection rates (0.066 m³/s, 0.132 m³/s, and 0.66 m³/s)

Figure 12. Influence of Pumping Rate: Hydraulic fracture networks generated for Example 2 with old and new crossing models for high viscosity fluid at injection rates from Table 3

4.3. Barnett example

To further validate the model in a realistic field condition, we examine a synthetic case that mimics the field example in Barnett Shale presented by Warpinski et al. [16] as shown in Figure 1. Though the details of the well and formation data and pumping schedule are not exactly replicated, the synthetic case is created using the data that is available in [16], so the well and formation configurations are very close to the real case.

Some of the critical information for fracture simulation, including Young's modulus and description of the natural fractures, is prescribed based on the work by Gale et al. [27]. According to [27], the Young's modulus for Barnett Shale is 33 GPa (4.8 x 10^6 psi). The natural fractures contain a dominant set trending West-Northwest direction (approximately North 70° West). There is also another set trending North-South direction. The hydraulic fractures in Barnett trend in the Northeast-Southwest direction. The natural fractures are mostly sealed and filled with calcite. Only largest fractures may be open and largest fracture clusters are expected to space couple hundred feet apart. To construct the natural fractures for UFM simulation, we assume that only the largest natural fractures contribute to the complex fracture network development. The exact values of fracture spacing and fracture length are difficult to determine. We make the assumption that the average fracture spacing is 100 ft and average fracture length is 200 ft. Only the dominant set of fractures is assumed. Figure 13 shows the top view of the well configuration, perforation clusters and the 2D traces of the generated natural fractures. The well geometry closely mimics the field case as shown in Figure 1.
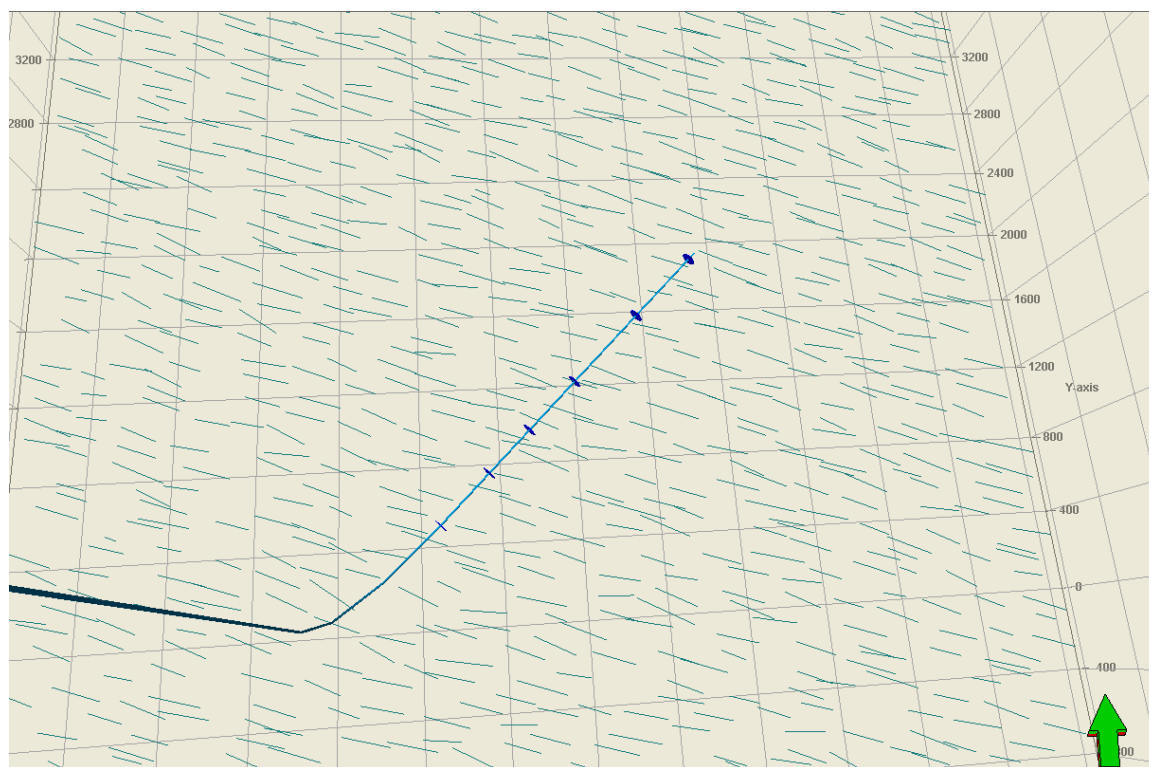

Figure 13. Top view of the wellbore, perforations and the natural fractures used for the Barnett simulations

For the complex fracture simulation, detailed vertical stress profile is not available from [16]. Instead a fixed height model is used based on the microseismic measurements presented in [16]. It is assumed that the fracture height is 310 ft covering Lower Barnett for the case of cross-linked gel treatment, and 360 ft for the slick water treatment. For the simulation of slick water refrac, any potential effect of previous cross-linked treatment and the small slick water treatment prior to the main treatment is not considered. Furthermore, a difference between maximum and minimum horizontal stress is assumed to be 200 psi. Table 4 shows the main parameters used for the fracture simulations.

Parameters	Xlink Gel treatment	Slick Water treatment
Young's modulus	4.8×10^6 psi	
Natural fracture direction	Average N70˚W, standard deviation 5˚	
Natural fracture length	Average 200 ft, standard deviation 40 ft	
Natural fracture spacing	Average 100 ft, standard deviation 20 ft	
Coefficient of friction	Average 0.6, standard deviation 0.1	
Hydraulic fracture direction	N40˚E	
Minimum horizontal stress	5324 psi	
Maximum horizontal stress	5524 psi	
Fracture height	310 ft	360 ft
Fluid rheology	n' = 0.42, k' = 0.002 lb-s/ft^2	1 cp
Injection rate : Q	70 bpm	125 bpm
Pump time	174 min	386 min
Proppant volume	715,000 lbs	600,000 lbs

Table 4. Input data for Barnett Shale case

Figure 14 shows the UFM simulated fracture geometry and width for both gel and slick water fracs at the end of the treatments.

Planar hydraulic fractures first initiate from the perforations. These fractures propagate as longitudinal fractures since the wellbore direction is closely aligned with the fracture orientation. For the cross-linked gel treatment, as these initial longitudinal fractures intersect the natural fractures that are approximately orthogonal to the fracture direction, the OpenT crossing model mostly predicts crossing through the natural fractures. Only when the fluid pressure is sufficiently high to exceed the normal stress acting on the natural fractures, do the natural fractures be opened up and accept fracturing fluid. The overall geometry predicted by UFM model shows a strong planar trend along the well with very narrow network width, consistent with the microseismic observation shown in Figure 1a.
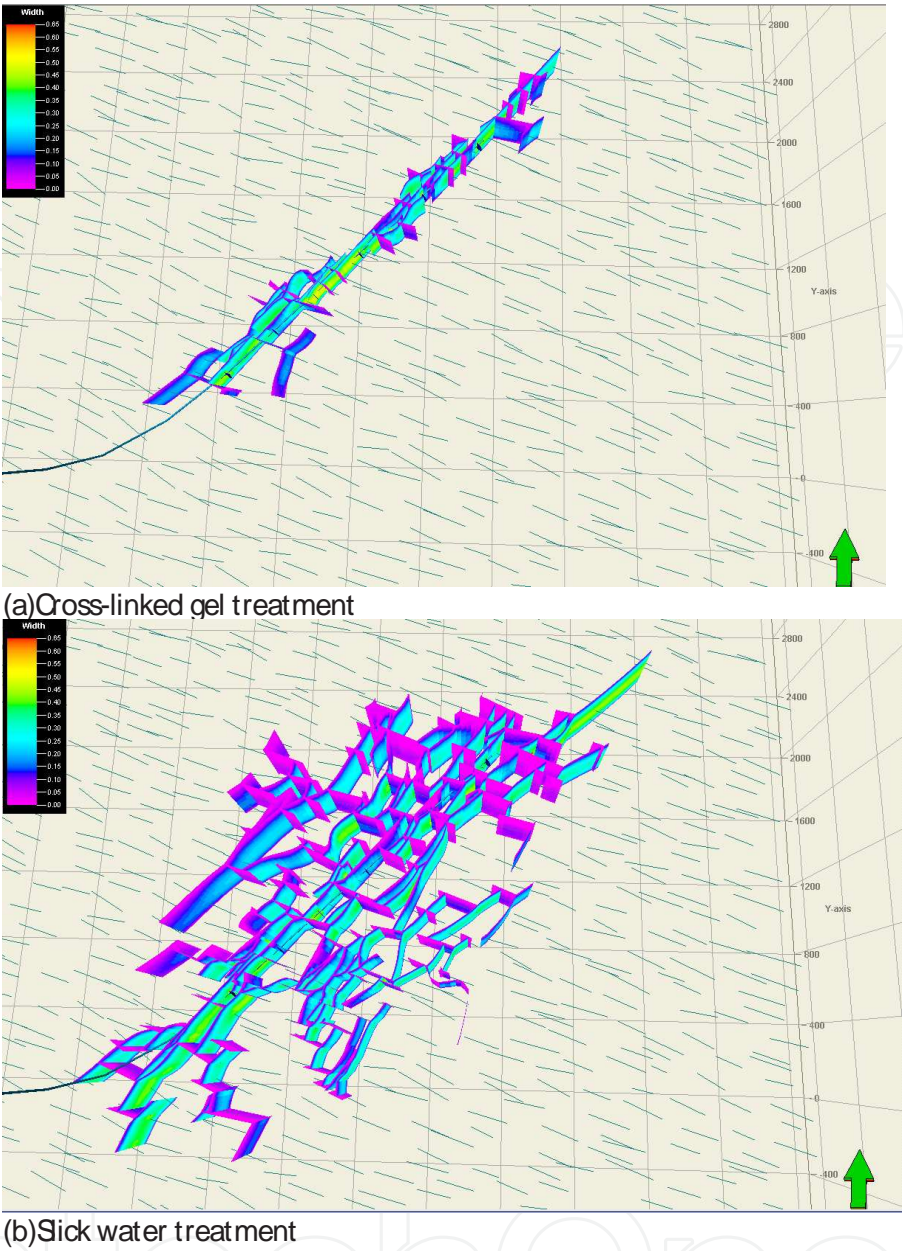
(a) Cross-linked gel treatment

(b) Slick water treatment

Figure 14. UFM simulation results for the Barnett case

For the slick water treatment, the OpenT crossing model mostly predicts non-crossing condition when a hydraulic fracture intercepts a natural fracture. This results in a much wider fracture network width as the fractures branch out as shown in Figure 14b. The width of the network is approximately 1700 ft wide, approximately the same as indicated by the micro-seismic data as shown in Figure 1b.

Example presented on Figure 14 showing the difference in HFN from two treatments with different types of fluid, matches microseismic cloud trend observed in [16] and definitely shows ability of UFM simulator with new implemented crossing model correctly predict hydraulic fracture complexity in naturally fractured formation.

5. Possible impact on production forecast

Unconventional Fracture Model (UFM) presents a powerful tool to evaluate hydraulic fracture network propagation under the specified field pumping conditions and can be used to predict developed hydraulic fracture network and match it with observed microseismic event cloud. The proper understanding of the fracture footprint as well as propped fracture surface estimation is an important input for the production evaluation. Because the OpenT crossing model predicts some changes in crossing patterns with different fluids used, it is important to understand the impact it could have on the production evaluation.

This section illustrates how the crossing criterion can influence the production. It presents simulation results of a fracturing-to-production simulation. The production part is done with the UPM model [28]. The base case for this Example 3 is from the paper [29] (Table 5).
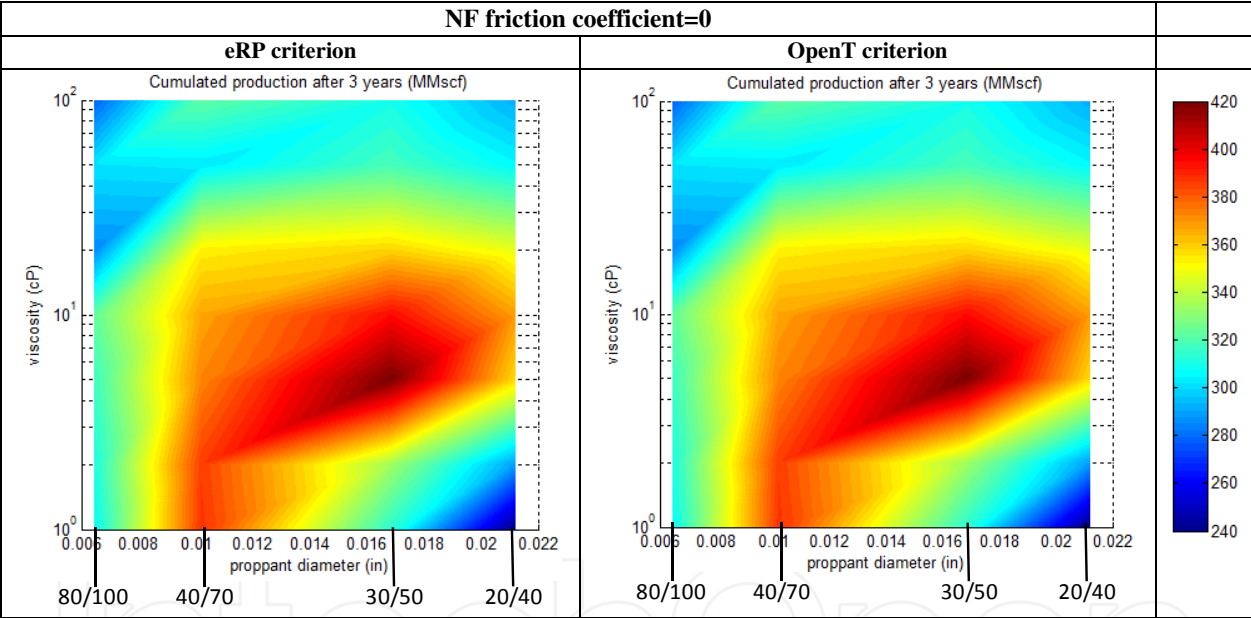

Figure 15. Cumulated production after 3 years for the two crossing criterion and a friction coefficient at NF = 0, as a function of the fracturing fluid viscosity and the proppant size

Figure15 shows the cumulated production after 3 years as a function of the proppant size and the fracturing fluid viscosity for the case when zero friction coefficient at NF is used and the two crossing models are applied. From Figure 15 we see that if there is no friction at the natural fractures, there is no difference between results from the two crossing criteria for this case. The reason is that if friction coefficient for the natural fracture is zero, both crossing criteria show that HF will not cross NF. The HFN footprint and fracture conductivity (identical when using both crossing criteria with zero friction coefficient) are shown at Figure 16 a,b for cases of slick water and more viscous fluid pumped.

Injection rate	0.21 m³/s
Number of Perforated Intervals	4
Stress anisotropy	0.3 MPa
Young's modulus	1.3×10^{10} Pa
Poisson's ratio	0.23
Fluid viscosity	0.001-0.1 Pa-s
Min horizontal stress	28.47 MPa
Max horizontal stress	28.76 MPa
Fracture toughness	1.5 MPa-m$^{0.5}$
Tensile strength	3.4MPa
NF friction Coefficient	0 -0.75
NF permeability	1 Darcy

Table 5. Input data for Example 3

If HF cannot cross NF, it is easier for slick water to penetrate and open NFs than for more viscous fluid, so HFN is generally more extended (Figure 16a left). While for the case of more viscous fluid it takes more time to open NF, HFN pattern is smaller (Figure 16)

When friction coefficient at NF is increased from 0 to 0.75, the output changes depending on the type of fluid pumped. The cumulated production forecast looks different for two crossing criteria used (Figure17).

For slick water treatments (Figure 18), eRP criterion shows some crossing of NFs (Figure18 left), while OpenT claims that no crossing should occur for slick water treatments (Figure 18 right). This difference in crossing models, produces considerable differences in production prediction after 3 years for low viscosity fluid treatments (Figure 17). It is important to mention, that it is a common observation that low viscosity fluids usually do not cross NFs, mainly because it is easier for them to penetrate to NF and open it [9]. The eRP criterion cannot capture this effect, while OpenT model correctly predicts HF/NF interaction for slick water case with friction coefficient at NF of 0.75.

When more viscous fluid pumped, results also show some differences (Figure19). With both criteria some crossing is observed, but OpenT in this case predicts more crossing than eRP criterion. Mention, that differences in results from eRP criterion for slick water and 100cP fluid are due to some differences in interaction angles between HF and NFs due to change in fluid properties, fluid pressure and due to stress shadow effect.

Due to small stress field anisotropy, the differences in production prediction for more viscous fluid are not significant (Figure 17), but still visible.
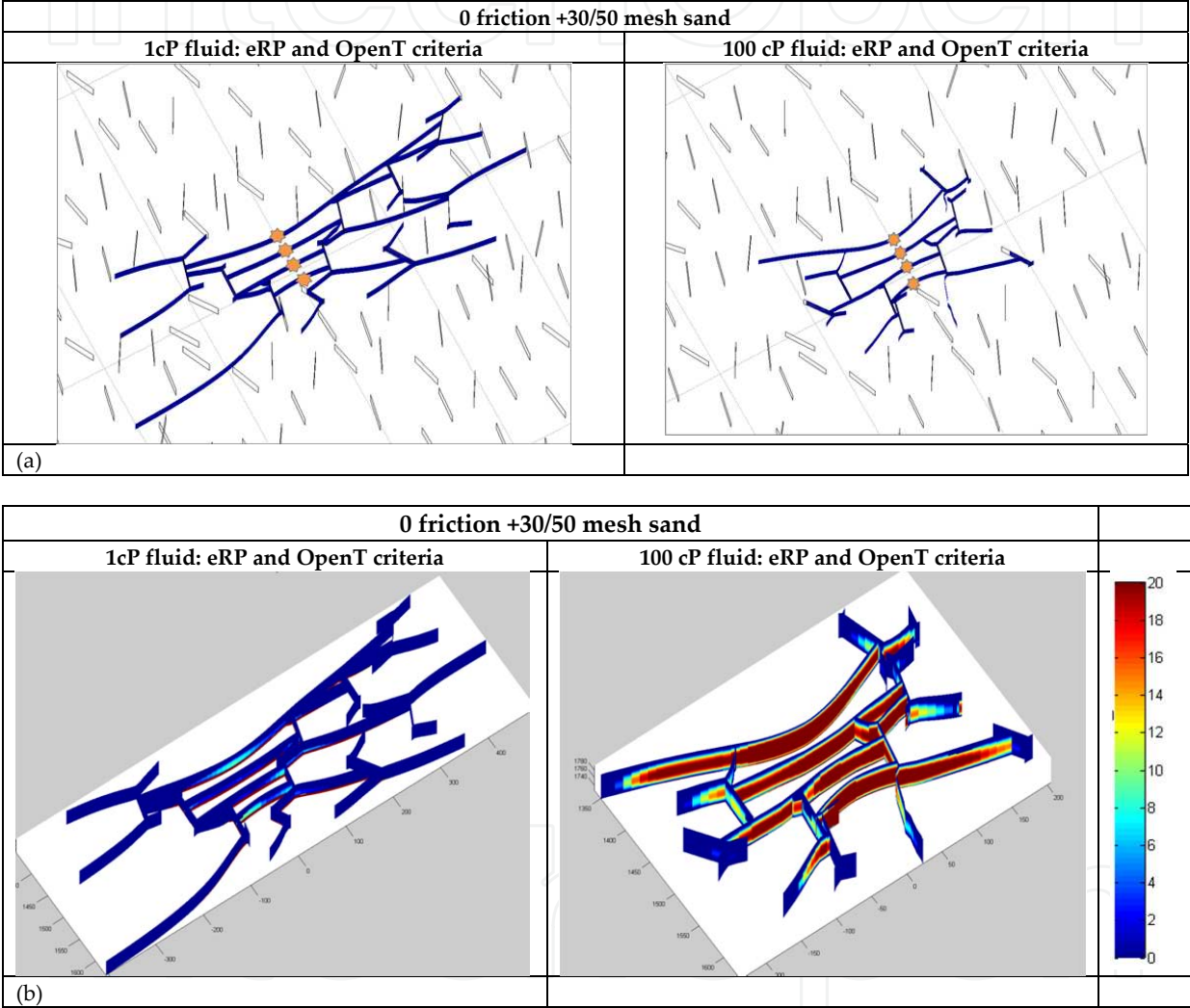
Figure 16. (a). HFN footprint for two types of fluid (with 30/50 mesh sand) for zero friction coefficient at NF. Both criteria show the same HFN footprint. (b). Fracture conductivity for two types of fluid (with 30/50 mesh sand) for zero friction coefficient at NF. Both criteria show the same HFN footprint
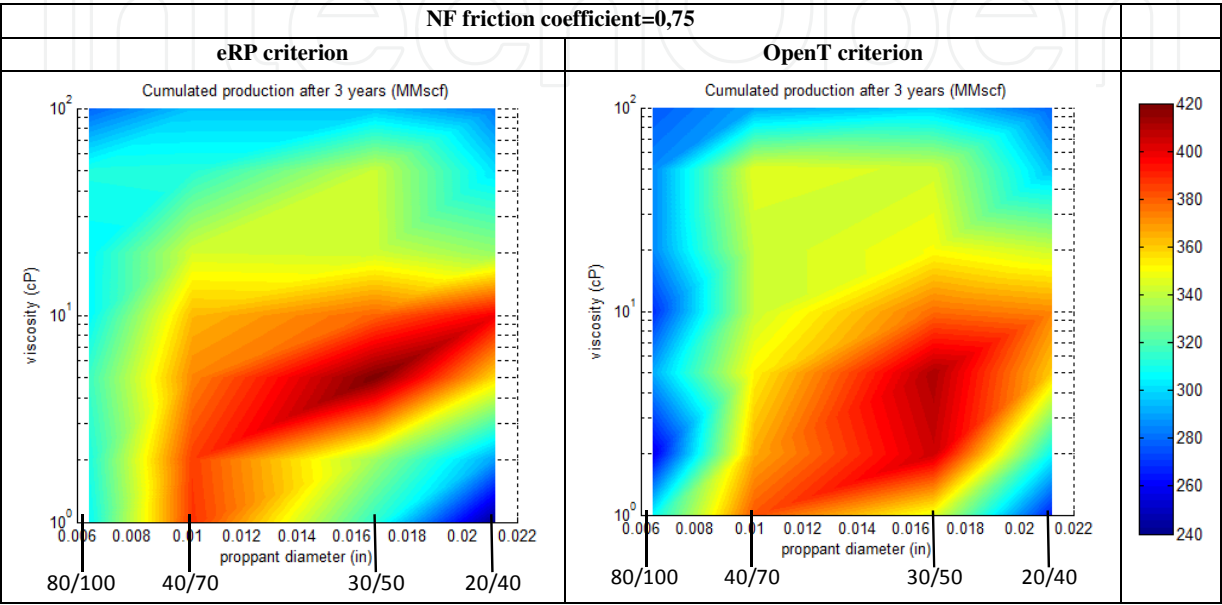
Figure 17. Cumulated production after 3 years for the two crossing criteria and a friction coefficient at NF of 0.75, as a function of the fracturing fluid viscosity and the proppant size

The main conclusion related to presented production examples, is that the difference between the two crossing criteria seems to be maximum for low viscosity fluid (slick water) and large proppant (30/50). This observation is expected because the lower the viscosity, the longer the fracture length and the stronger interaction with NF are. Also, eRP criterion shows some crossing of NFs for slick water case, while OpenT shows no crossing, and larger proppants are more sensitive to fracture intersections. The fracture width is larger if the HF does not cross NF and slurry propagated inside the NF with a larger normal stress (in case of stress anisotropy) and smaller width, thus increasing the likelihood of bridging. Also, the less crossing occurs, the more time HF needs to spend stopped at NF before building enough pressure to overcome the stress anisotropy and resume propagating inside the NF for high viscosity fluids. In this case, more proppant will settle close to the perforations, reducing the propped length and thus the production.
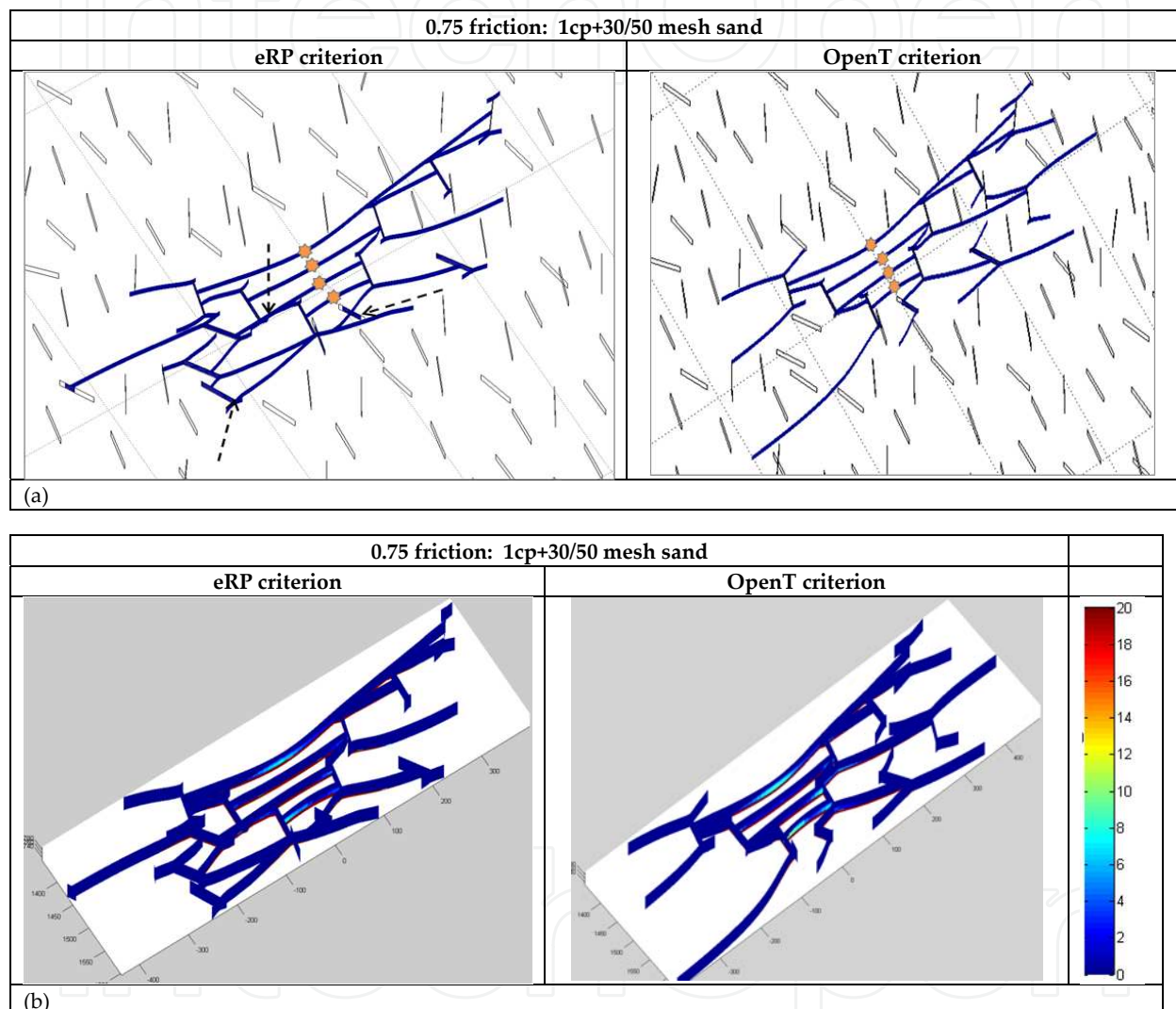
Figure 18. (a). HFN footprint for slick water (with 30/50 mesh sand) for friction coefficient at NF=0.75. Both criteria show similar HFN footprint. eRP shows some crossing (shown by dashed arrows), while OpenT shows no crossing for slick water case (b). Fracture conductivity for slick water (with 30/50 mesh sand) for friction coefficient at NF=0.75
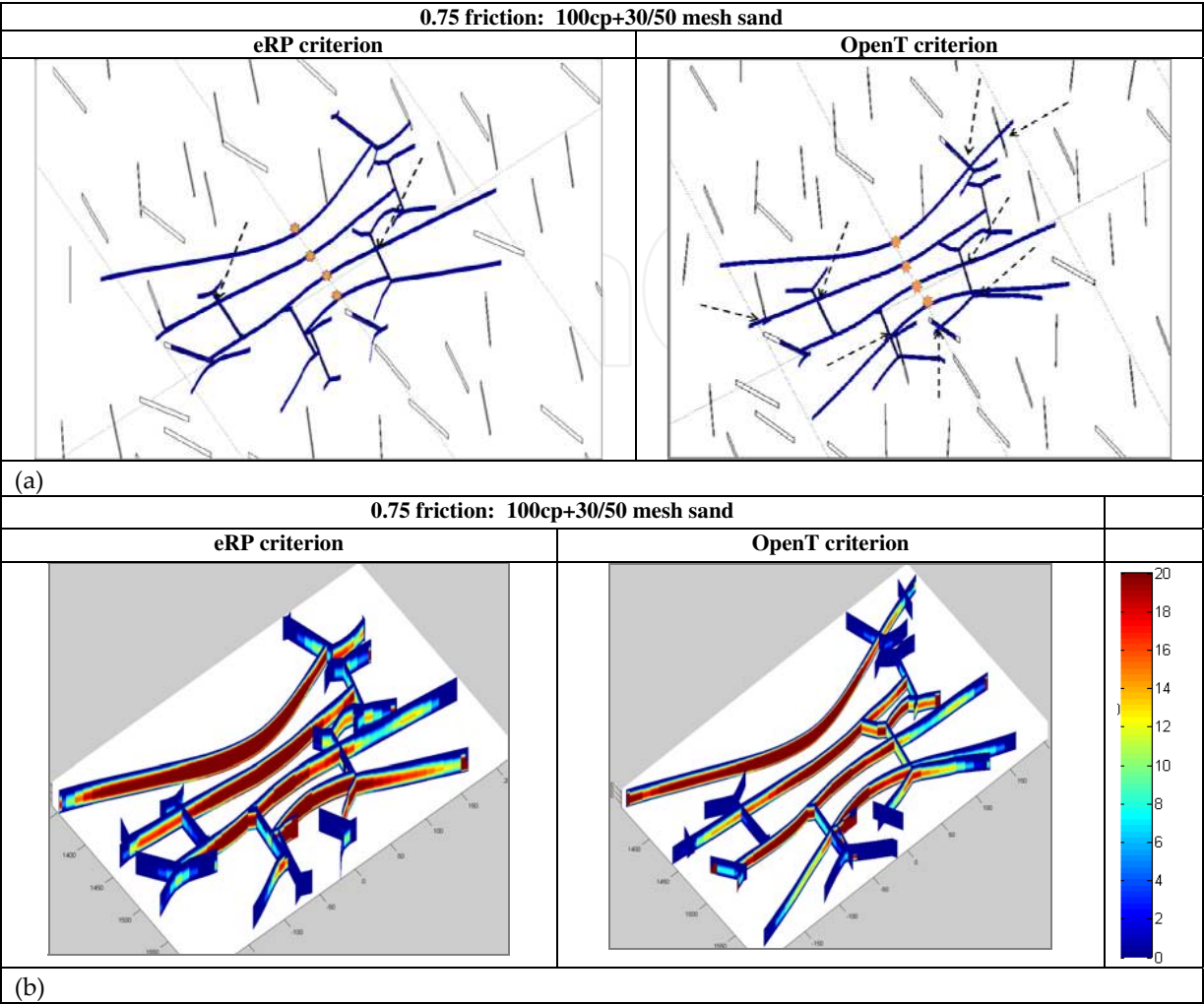
Figure 19. (a). HFN footprint for 100cP viscosity fluid (with 30/50 mesh sand) for friction coefficient at NF=0.75. Arrows point at crossing (b). Fracture conductivity for 100cP viscosity fluid (with 30/50 mesh sand) for friction coefficient ant NF=0.75

6. Conclusions

A new crossing model (OpenT) which takes into account fluid properties, properties of the rock mass and natural fractures, have been developed, validated [20, 21], and implemented in UFM. The similarities and differences in fracture footprint predicted based on the OpenT model and eRP criterion have been demonstrated and discussed. OpenT crossing model shows more realistic results for some cases (as for the field and laboratory observations) than existing purely rock property based models.

While eRP model properly accounts for interaction angle, stress anisotropy, rock tensile strength and NF friction coefficient, the OpenT model accounts also for NF and fluid properties. The crossing prediction from OpenT criterion, and therefore corresponding HFN foot-

print, could be different for low viscosity fluids and high viscosity fluids, while eRP model shows similar crossing patterns for low and high viscosity fluids. In the mean time both criteria show similar results for some cases.

It is important to mention that whether HF will cross (dilate, or open) NF depends on the combined impact of rock properties (local stress field, tensile strength, toughness, etc), NF properties (permeability, toughness, friction coefficient, cohesion, etc), HF/NF interaction angle, fluid properties, injection rate and other properties.

In general, the Unconventional Fracture Model (UFM) with new OpenT crossing model provides more reliable results to predict and evaluate hydraulic fracture network geometry and improve production forecast. The Barnett Shale example presented in Figure 14 shows the differences in HFN from two treatments with two different types of fluids. The predicted results closely match the microseismic cloud observed in [16] and show the ability of UFM simulator with the new crossing model (OpenT) to correctly predict hydraulic fracture complexity in naturally fractured formation.

Acknowledgements

Author details

Olga Kresse[1*], Xiaowei Weng[1], Dimitry Chuprakov[2], Romain Prioul[2] and Charles Cohen[1]

*Address all correspondence to: okresse@slb.com

1 Schlumberger, Sugar Land, USA

2 Schlumberger Doll Research, Boston, USA

References

[1] Chuprakov DS, Akulich AV, Siebrits E, Thiercelin M. Hydraulic Fracture Propagation in a Naturally Fractured reservoir. SPE 128715, Presented at the SPE Oil and Gas India Conference and Exhibition held in Mumbai, India, 20-22, January, 2010.

[2] Zhao J, Chen M, Jin Y, Zhang G. Analysis of fracture propagation behavior and fracture geometry using tri-axial fracturing system in naturally fractured reservoirs. Int. J. Rock Mech. & Min. Sci 2008; 45: 1143-1152.

[3] Thiercelin M, Makkhyu E. Stress field in the vicinity of a natural fault activated by the propagation of an induced hydraulic fracture. In: Proceedings of the 1st Canada-US Rock Mechanics Symposium 2007; 2:1617-1624.

[4] Zhang X, Jeffrey RG. The role of friction and secondary flaws on deflection and re-initiation of hydraulic fractures at orthogonal pre-existing fractures. Geophys J Int. 2006;166(3): 1454-1465.

[5] Zhang X, Jeffrey RG. Reinitiation or termination of fluid-driven fractures at frictional bedding interfaces. J Geophys Res-Sol Ea. 2008; 113(B8), B08416.

[6] Zhang X, Jeffrey RG, Thiercelin M. Effects of Frictional Geological Discontinuities on hydraulic fracture propagation. SPE 106111, Presented at the SPE Hydraulic Fracturing Technology Conference, College Station, Texas, January29-31, 2007.

[7] Zhang X, Jeffrey RG., Thiercelin M. Deflection and propagation of fluid-driven fractures as frictional bedding interfaces: a numerical investigation. Journal of Structural Geology 2007; 29: 390-410.

[8] Zhang X, Jeffrey RG, Thiercelin M. Mechanics of fluid-driven fracture growth in naturally fractured reservoirs with simple network geometries. Journal of Geophysical Research 2009;114, B12406.

[9] Beugelsdijk LJL, de Pater CJ, Sato K. Experimental hydraulic fracture propagation in a multi-fractured medium. SPE 59419, Presented at the SPE Asia Pacific Conference in Integrated Modeling for Asset Management, Yokohama, Japan, April 25-26, 2000.

[10] Renshaw CE, Pollard DD. An Experimentally Verified Criterion for Propagation across Unbounded Frictional Interfaces in Brittle, Linear Elastic-Materials. International Journal of Rock Mechanics and Mining Sciences & Geomechanics Abstracts. 1995 Apr, 32(3): 237-49.

[11] Warpinski NR., Teufel LW. Influence of Geologic Discontinuities on Hydraulic Fracture Propagation (includes associated papers 17011 and 17074). SPE Journal of Petroleum Technology 1987;39(2): 209-220

[12] Blanton TL. An Experimental Study of Interaction Between Hydraulically Induced and Pre-existing Fractures. SPE 10847, Presented at the SPE/DOE Unconventional Gas Recovery Symposium, Pittsburgh, PA, May 16-18, 1982.

[13] Blanton TL. Propagation of Hydraulically and Dynamically Induced Fractures in Naturally Fractured Reservoirs. SPE Unconventional Gas Technology Symposium; 01/01/1986; Louisville, Kentucky,1986.

[14] Gu H, Weng X. Criterion For Fractures Crossing Frictional Interfaces At Non-orthogonal Angles. 44th US Rock Mechanics Symposium and 5th US-Canada Rock Mechanics Symposium; 01/01/2010; Salt Lake City, Utah: American Rock Mechanics Association; 2010.

[15] Gu H, Weng X, Lund JB, Mack M, Ganguly U, Suarez-Rivera R. Hydraulic fracture crossing natural fracture at non-orthogonal angles, a criterion, its validation and applications. Paper SPE 139984 presented at the SPE Hydraulic Fracturing Conference and Exhibition, Woodlands, Texas, 24-26 January, 2011.

[16] Warpinski NR, Kramm RC, Heinze JR, Waltman CK. Comparison of Single- and Dual-Array Microseismic mapping Techniques in the Barnett Shale. SPE 95568. Presented at the 2005 SPE Annual Technical Conference and Exhibition, Dallas, Texas, October 9012, 2005.

[17] Cipolla C, Weng X, Mack M, Ganguly U, Gu H, Kresse O, Cohen C. Integrating Microseismic Mapping and Complex Fracture Modeling to Characterize Fracture Complexity. SPE 140185 Presented at the SPE Hydraulic Fracturing Technology Conference and Exhibition in The Woodlands, Texas, USA, January 24-26 2011.

[18] Gil I, Nagel N, Sanchez-Nagel M. The Effect of Operational Parameters on Hydraulic Fracture Propagation in Naturally Fractured Reservoirs – Getting Control of the Fracture Optimization Process. Presented at 45th US Rock Mechanics/ Geomechanics Symposium, San Francisco, CA, 26-29 June, 2011.

[19] Nagel N, Gil I, Sanchez-Nagel M, Damjanac B. Simulating Hydraulic Fracturing in Real Fractured Rock – Overcoming the Limits of Pseudo 3D Models. SPE 140480, presented at the SPE HFTC in Woodlands, Texas, USA, 24-26 January, 2011.

[20] Chuprakov D, Melchaeva O, Prioul R. Hydraulic Fracture Propagation Across a Weak Discontinuity Controlled by Fluid Injection. InTech; 2013.

[21] Chuprakov D, Melchaeva O, Prioul R. Injection-sensitive mechanics of hydraulic fracture interaction with discontinuities. Submitted for ARMA Symposium 2013.

[22] Kresse O, Cohen C, Weng X, Wu R, Gu H. Numerical modeling of hydraulic fracturing in naturally fractured formations. 45th US Rock Mechanics/ Geomechanics Symposium, San Francisco, CA, 26-29 June, 2011.

[23] Weng X., Kresse O., Cohen C., Wu R., Gu H. Modeling of Hydraulic Fracture Network Propagation in a Naturally Fractured Formation. Paper SPE 140253 presented at the SPE Hydraulic Fracturing Conference and Exhibition, Woodlands, Texas, USA, 24–26 January, 2011.

[24] Kresse O, Weng X, Wu R, Gu H. Numerical modeling of Hydraulic fractures interaction in complex Naturally fractured formations. ARMA-292, Presented at 46th US Rock Mechanics /Geomechanics Symposium, Chicago, Il, USA, 24-27 June 2012.

[25] Valko P, Economides MJ. Hydraulic Fracture Mechanics: John Wiley & Sons; 1995.

[26] Leguillon D. Strength or toughness? A criterion for crack onset at a notch. Eur J Mech a-Solid. 2002 Jan-Feb;21(1):61-72.

[27] Gale JFW, Reed RM, Holder J. Natural fractures in the Barnett Shale and their importance for hydraulic fracture treatment. AAPG Bulletin, v91, No. 4: 603-622, April 2007.

[28] Cohen CE, Xu W, Weng X, Tardy P. Production Forecast After Hydraulic Fracturing in Naturally Fractured Reservoir: Coupling a Complex Fracturing Simulator and a Semi-Analytical Production Model. SPE paper 152541 presented at the SPE Hydraulic Fracturing Technology Conference and Exhibition held in The Woodlands, Texas, USA, 6-8 February 2012.

[29] Cohen CE, Abad C, Weng X, England K, Phatak A, Kresse O, Nevvonen O, Lafitte V, Abivin P. Analysis on the Impact of Fracturing Treatment Design and Reservoir Properties on Production from Shale Gas Reservoirs. IPTC 16400, Presented at the International Petroleum Technology Conference, Beijing, China, 26-28 March, 2013.